Nanotechnology for Environmental Engineering (2023) 8:131–142
https://doi.org/10.1007/s41204-021-00214-0

ORIGINAL PAPER

Nanochitosan impregnated polyurethane foam in the removal of phosphate and coliforms from greywater

Anjali P. Sasidharan[1] · V. Meera[1] · Vinod P. Raphael[2]

Received: 19 September 2021 / Accepted: 30 December 2021 / Published online: 2 February 2022

Abstract

The study was mainly intended to explore the feasibility of application of nanomaterials in greywater treatment, an area that has not been investigated till now. A newflanged sorbent by impregnating chitosan nanoparticles on polyurethane foam (PFC) was developed for phosphate and coliform removal from greywater. The nanoparticle formation was first established by the absorbance peak at 280 nm with the ultraviolet–visible spectrum and the field emission scanning electron microscopic images recognised the spherical nanoparticles with size 56–112 nm. The point of zero charge was found to be 7.4. The functional group beneficial for the uptake of phosphate and coliforms was unveiled by the Fourier transform infrared spectroscopic analysis. X-ray diffraction analysis of PFC revealed the stability of the sorbent by providing nearly the same pattern before and after treatment, and the presence of specific elements (C, O, P) in PFC was determined by energy-dispersive X-ray spectroscopy. The experimental studies showed that at optimised operating conditions, PFC removed 26.15% of phosphate (influent phosphate concentration of 155 mg/L) within 6 h and 99.91% of coliforms (influent coliform concentration of 38×10^3 CFU/mL) within 1.5 h from the synthetic greywater. The phosphate sorption by PFC was described by monolayer adsorption and pseudo-second-order kinetics. The multiple regression analysis of sorption data with IBM SPSS statistics 26.0 showed an R^2 value of 0.959. The bacterial growth inhibition efficiency obtained for PFC was 77.53% in an inoculated broth solution with a coliform count of 5×10^6 CFU/mL. PFC can therefore be considered a potent sorbent for coliforms with high antibacterial activity. Since the phosphate removal was not high, further modification of PFC by metal/metal oxide nanoparticles which possess high phosphate adsorption capacity may enhance the efficacy.

✉ V. Meera
vmeera@gectcr.ac.in

[1] Department of Civil Engineering, Government Engineering College, Thrissur, APJ Abdul Kalam Technological University, Thiruvananthapuram, Kerala, India

[2] Department of Chemistry, Government Engineering College, Thrissur, APJ Abdul Kalam Technological University, Thiruvananthapuram, Kerala, India

Graphical abstract

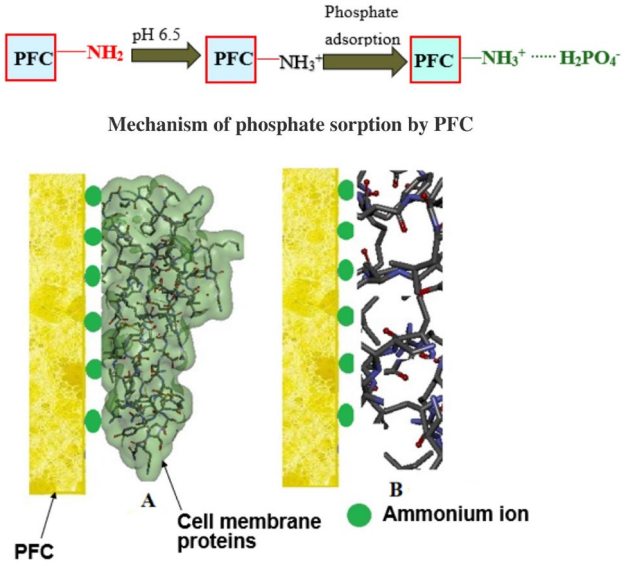

Keywords Bactericidal property · Chitosan nanoparticles · Impregnation · Isotherm · Kinetics · Polyurethane foam

Introduction

Water quality has been adversely affected by the increasing population density and land-use changes. Among the major water pollution problems, eutrophication and bacterial contamination have gained great interest globally [1]. The high amount of phosphate release from the wastewater of urban areas, industrial activities, or agricultural activities causes eutrophication and depletes the dissolved oxygen levels. The excessive phosphate levels in water make it unsuitable for human consumption and recreation. The phosphate concentration above 1 mg P/L results in osteoporosis and kidney damage [2, 3]. The existing treatment systems in removing phosphate like membrane filtration, reverse osmosis, electrodialysis, coagulation, etc. have various shortcomings like increased cost, dependability, and sludge handling. The biological treatment systems become effective only at phosphate levels that maintain the proper metabolism of microorganisms [4, 5]. A simple, quick, adaptable, and effective phosphate removal method even at low phosphate concentration is therefore necessary.

The microbial quality of the surface water gets threatened by the discharge of domestic and industrial wastewater. The microbiological risks depend on the amount of pathogenic concentration and the usage of water [6]. The presence of bacteria, viruses, and protozoa in water results in various water-borne diseases like cholera, dysentery, typhoid, etc. Total coliforms are one of the most commonly used microbial indicators of pathogenic pollution. Conventional disinfection methods include chlorination, ozonation, and ultraviolet (UV) radiation. Although these methods can beneficially control pathogenic organisms, the production of dangerous disinfection by-products (DBPs) by chlorination, and the difficulty and cost of operating ultraviolet radiation and ozonation, leads to an urgent need for the development of new promising materials [7].

The reuse of wastewater helps to lower the freshwater extraction from rivers and aquifers. A large quantity of greywater is produced from domestic activities such as laundry, dishwashing, and bathing. The quantity and characteristics of this waste vary depending on the socio-economic status, cooking habits, cultural practices, cleaning agents used, and demography. The treated greywater can be a reliable source of water and can be reused in irrigation, toilet flushing, etc. Greywater treatment for reuse has gained momentum in India and is used widely in multi-storied buildings like hospitals, apartments, etc. But the existing treatment methods often fail to remove phosphate and coliforms effectively from greywater [8].

Adsorption is one of the most promising technologies that may provide a solution to challenging water/wastewater problems and is greatly affected by temperature [9]. But

the adsorption processes by conventional means needs to be improved due to their high capital cost, ineffectiveness, and reduced selectivity [10]. The increased effectiveness of nanosorbents has opened the way towards the advanced water/wastewater treatment system. The high reactivity and degree of functionality, size-dependent properties, and large specific surface area of nanosorbents make them preferable to conventional sorbents [11–13]. Chitosan nanoparticles outperform various other nanomaterials in terms of stability, sorption capacity, and antibacterial activity [14]. Nanochitosan can be easily prepared by the ionic gelation method with sodium tripolyphosphate as a cross-linker. The cross-linking helps to maintain stability at different pH conditions. The excellence of nanochitosan in water/wastewater treatment is mainly due to the presence of reactive amino and hydroxyl groups. Also, the amorphous nature of nanochitosan enhances the sorption capacity [15, 16]. Even though the nanoparticles are efficient in removing various pollutants from water, their aggregation will result in reduced efficacy. Immobilisation of nanoparticles on a suitable support such as sand, polyurethane foam, zeolite, and fibreglass improves the stability and increases their practical application [17]. The biocompatibility and mechanical properties of polyurethane foam make it a different polymer from others and is commonly used for various applications [18]. The polyurethane foam exhibits high porosity with large specific surface area. Also, the carbamate group of polyurethane foam binds the surface of nanoparticles [19].

This study dealt with the investigations on the potency of nanochitosan impregnated polyurethane foam (PFC) in eliminating phosphate and coliforms from synthetic greywater. The sorbent characterisation was done using the field emission scanning electron microscopy (FESEM), point of zero charge, Fourier transform infrared (FTIR) spectroscopy, X-ray diffraction (XRD) studies, and energy-dispersive X-ray (EDX) spectroscopy. The impact of various parameters (contact time, adsorbent dosage, pH,) affecting the phosphate sorption and reusing capability of the sorbent were studied. In addition, the isothermal and thermodynamic behaviour of the phosphate sorption process and kinetics was verified. The experimental data were analysed and modelled using IBM SPSS statistics 26.0. Coliform removal efficacy was evaluated at different contact time and pH with optimised sorbent dosage for phosphate removal. The antibacterial activity of PFC was also assessed. The application of nanoparticles in the field of greywater treatment and the use of nanochitosan for phosphate removal have not been yet explored.

Materials and methods

Materials

The entire study was conducted using analytical-grade chemicals. The reagents sulphuric acid (H_2SO_4), ascorbic acid, sodium acetate trihydrate ($CH_3COONa.3H_2O$), glucose, potassium dihydrogen phosphate (KH_2PO_4), disodium hydrogen phosphate (Na_2HPO_4), sodium hydroxide (NaOH), hydrochloric acid (HCl), ammonium molybdate ($(NH_4)_6Mo_7O_{24}.4H_2O$), magnesium sulphate ($MgSO_4$), antimony potassium tartrate ($KSbOC_4H_4O_6.1/2H_2O$), ammonium chloride (NH_4Cl), nutrient broth, plate count agar, and M-Endo medium were supplied by Merck Millipore. Coliform bacterial culture was obtained from the College of Veterinary and Animal Sciences, Mannuthy, Kerala, India.

Sorbent preparation and instrumental analysis

The method adopted in the synthesis of chitosan nanoparticles (CSNPs), formation of the sorbent by impregnating nanochitosan on polyurethane foam (PFC), and the characterisation techniques (UV–Vis spectroscopy, FESEM, EDX, FTIR, XRD, and point of zero charge) have been reported in the previous study [20]. Briefly, chitosan nanoparticles (CSNPs) were prepared by dissolving chitosan (CS) in acetic acid which was then allowed to undergo ionic gelation with sodium tripolyphosphate (TPP) under magnetic stirring. The nanoparticle formation was realised by the appearance of solution in opalescent nature [21, 22]. The synthesised CSNPs were soaked in the polyurethane form (PUF) for 24 h and dried after draining out excess solution [23, 24]. The PFC was thoroughly washed and stored for future use.

Studies on phosphate sorption under batch mode

The feasibility of PFC in sorbing phosphate from synthetic greywater was studied under batch equilibrium conditions. The influence of contact time, pH, and sorbent dosage on removing phosphate from synthetic greywater was studied. The greywater was prepared artificially with sodium acetate trihydrate (400 mg/L), glucose (300 mg/L), ammonium chloride (225 mg/L), potassium dihydrogen phosphate (75 mg/L), disodium hydrogen phosphate (150 mg/L), and magnesium sulphate (50 mg/L) [25].

The investigations were done by varying contact time from 1 to 7 h (1 h interval) and 24 h at pH 6 and sorbent dosage 3 g/L; pH from 4 to 11 using 1 N HCl / 1 N NaOH

at different contact time (1–6 h) and sorbent dosage 3 g/L; the dosage of sorbent was varied from 0.5 to 4 g/L at optimised pH and contact time. The reuse capacity of the sorbent by eluting phosphate with NaOH was examined. The adsorption kinetics and isotherm were established.

Phosphate sorption efficiency by PFC(%)is given by,

$$E = \frac{(C_0 - C_t)}{C_0} \times 100 \quad (1)$$

$$\text{Sorption capacity(mg/g)is calculated by, } q_t = (C_0 - C_t) \times \frac{V}{m} \quad (2)$$

where C_0 (mg/L) and C_t (mg/L) are the influent and effluent concentration of phosphate at any time t, respectively, V represents the sample volume in *L*, and *m* (g) is the mass of sorbent.

The pseudo-first-order and pseudo-second-order kinetic models were used for studying the kinetics of phosphate sorption. The experimental data of phosphate sorption with various sorbent dosages were used for isothermal modelling with Langmuir, Freundlich, and D–R isotherms. The assessment of the best fit kinetics and isotherm model was done by using the higher value of correlation coefficient (R^2) and lower value of Chi-square (χ^2).

Statistical interpretation of phosphate sorption data

The statistical analysis of experimental data of phosphate removal efficacy was done with IBM SPSS statistics 26.0 (95% confidence interval). The relation between independent variables (contact time, pH, and adsorbent dosage) and the dependent variable (phosphate removal efficiency) was formed using regression analysis. The model verification was done by the value of R^2 (coefficient of determination), ANOVA results and normalised root mean square error (NRMSE) value.

$$NRMSE = \left[\frac{\sum_{i=1}^{n}(E_m - E_e)^2}{nE^2}\right]^{0.5} \quad (3)$$

where the phosphate removal efficiency predicted by the model is represented by E_m and the phosphate removal efficiency got from the experiment is denoted by E_e. The average of E_e is represented by *E*. NRMSE will be less than 10% for an excellent model, 10–20% for a good model, 20–30% for a fair model, and greater than 30% for a poor model [26].

Assessment of antibacterial activity and coliform removal efficacy of PFC

The bactericidal property was evaluated by measuring the optical density of the inoculated broth solutions containing coliforms and sorbents (PFC and PUF) using UV–Vis spectrophotometer at 600 nm [27]. The analysis was done with a coliform bacterial suspension containing 5×10^6 CFU/mL. 40 mL of the nutrient broth (prepared by suspending 13 g of nutrient broth in 1000 mL of distilled water) was added to a conical flask of 250 mL capacity which was inoculated with 1 mL of the coliform bacterial suspension. The sorbents PUF and PFC (0.6 g) were added to another flask containing nutrient broth and bacterial feed. After incubation at 35 °C for 18 h, optical densities (OD) of suspensions were taken using the spectrophotometer at 600 nm. The incubated nutrient broth (without adsorbents) was taken as the reference.

The effectiveness of PFC in removing coliforms at varying pH from 5 to 9 and contact time 0.5–3 h was also assessed. The coliform bacterial suspension was inoculated to synthetic greywater composition to get an influent concentration of 38×10^3 CFU/mL. The coliform count was measured using the membrane filter technique [28].

Results and discussion

Sorbent characterisation

The UV–Vis spectrum of CSNPs showed the highest absorption peak at 280 nm. The size of nanoparticles obtained from FESEM images was in the range of 56–112 nm and showed agglomeration. The FESEM images of CSNPs (Figure S1A), PUF (Figure S1B), and PFC (Figure S1C) are included in the supplementary material section. The impregnation of nanochitosan on PUF resulted in non-agglomeration (Figure S1C). The cross-linking of ammonium group of CS and TPP for the formation of CSNPs along with the characteristic functional groups of CS, CSNPs, and PUF was exposed by the FTIR spectrum of CS (Figure S2A), CSNPs (Figure S2B), and PUF (Figure S2C). The FTIR spectroscopic studies of PFC (Fig. 6) revealed the role of NH group of PUF during the impregnation of CSNPs, and the existence of free amino group (NH stretching vibration at 3284.68 cm^{-1} and NH bending vibration at 1628.47 cm^{-1}) favourable for the sorption of phosphate and antibacterial activity. The non-crystalline nature of CSNPs and PUF was verified by their XRD pattern in Figure S3A and B, respectively. The CSNPs and PUF retained their non-crystalline nature after impregnation as shown in the XRD pattern of PFC (Fig. 7). The presence of CSNPs on the surface of PFC was confirmed by the EDX pattern (Fig. 8). The surface charge of PFC

obtained from the point of zero charge study showed that the favourable pH for anionic sorption was below 7.4. The plot of point of zero charge (Figure S4) is given in the supplementary material section.

Characteristics of synthetic greywater

The characteristics of synthetic greywater used in the study are shown in Table 1.

Batch studies on the removal of phosphate from synthetic greywater

Influence of contact time

The experiments were carried out in synthetic greywater at pH 6 and adsorbent dose 3 g/L. For an increase in contact time from 1 to 6 h, the phosphate removal efficacy increased from 10.02 to 25.65% (Fig. 1A). The phosphate removal efficacy increased rapidly at the initial phase (1–3 h), after which showed a slow uptake till reaching the equilibrium at 6 h. This trend can be described by the abundant unoccupied adsorption sites at the beginning of the sorption process. Thereafter, the adsorbed ions cause electrostatic repulsion, resulting in reduced accessibility of the remaining sites [12, 16, 29–31].

Table 1 Characteristics of the synthetic greywater used in the study

Parameters	Concentration
COD	254.00 mg/L
BOD	168.00 mg/L
pH	6.16
Phosphates	155.00 mg/L
TDS	0.71 ppt
Total coliforms	38×10^3 CFU/mL

Influence of pH

The pH of synthetic greywater was varied from 4 to 11, for different contact time (1–6 h) with sorbent dosage of 3 g/L. The removal of phosphate by PFC increased with pH from 4 to 6.5 and decreased with further increase in pH. This was mainly related to the positive surface charge of sorbent at acidic pH, resulting in more phosphate sorption. The repulsive action between phosphate and hydroxyl ions resulted in reduced efficacy at higher pH [30, 32]. The maximum phosphate removal efficiency of 26.15% was obtained at pH 6.5 (Fig. 1B). The point of zero charge highlighted the positive surface charge possessed by the sorbent at pH 6.5 which favours the sorption of anions. Moreover, at pH 6.5, the phosphate ions exist in the form is $H_2PO_4^-$, most favourable for getting sorbed [33]

Influence of adsorbent dosage

The impact of adsorbent dosage on phosphate sorption was evaluated by varying dosage from 0.5 to 4 g/L at pH 6.5 and contact time 6 h. With increasing sorbent dosage, the percentage of phosphate sorption also increased. This is ascribed to the accessibility of more sorption sites. However, the increase in the amount of sorbent above the optimal did not make any significant increase in phosphate sorption. This might be due to the exposure of all active sorption sites at lower doses, while higher doses resulted in sorbent aggregation, and thus, only a fraction of active sites get exposed [9, 15, 16, 29]. At the optimum dosage of 3 g/L, the phosphate removal efficacy was found to be 26.15%, whereas the efficiency was 3.53% for PUF. The results are depicted in Fig. 2.

The percentage removal of phosphate from synthetic greywater by PFC was not high, which may be due to the existence of coexisting anions and organic matter. The presence of coexisting ions like chloride (150 mg/L), sulphate (40 mg/L),

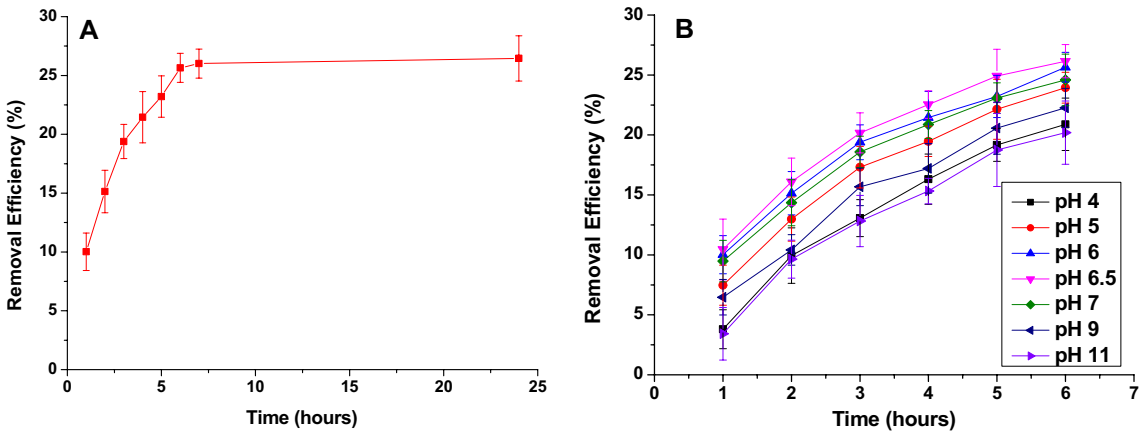

Fig. 1 Influence of **A** contact time and **B** pH on the removal of phosphate by PFC

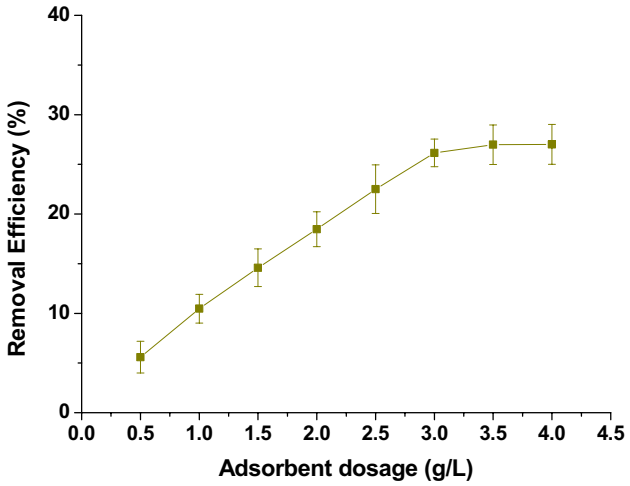

Fig. 2 Influence of adsorbent dosage on phosphate removal by PFC

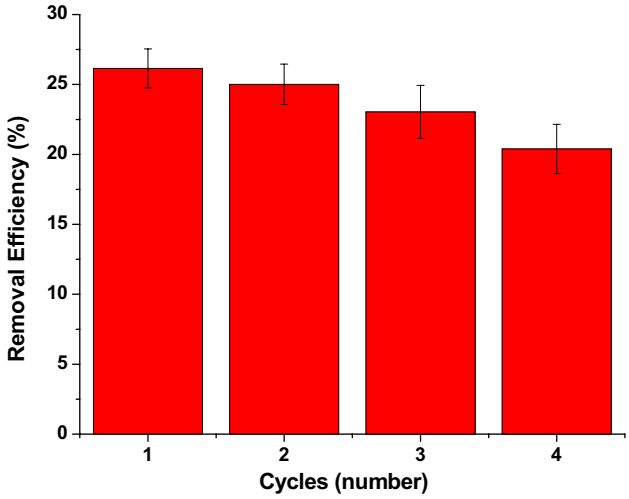

Fig. 3 Reusing capacity of PFC in four adsorption/desorption cycles

bicarbonates (100 mg/L) in the synthetic greywater compete with phosphate ions for adsorption [32]. The organic matter like glucose will increase the negative charge on the sorbent surface and restrict the sorption of phosphate [34]. The high phosphate concentration in the synthetic greywater also resulted in reduced efficacy.

The efficacy of PFC in removing phosphate can be enhanced by the incorporation of metal nanoparticles (silver, zinc, copper, titanium). The amino group of nanochitosan can form stable complexes with metal/metal oxide nanoparticles which are favourable for anionic sorption [35].

Reusing capacity of PFC

The sorbent capacity for reusing was assessed at pH 6.5 and contact time 6 h. The sorbents were regenerated by treating with 0.01 M, 0.1 M, and 0.5 M NaOH solution for 24 h. The phosphate desorption percentages were 34.9%, 65.5%, and 67.1% for 0.01 M, 0.1 M, and 0.5 M NaOH solutions, respectively.

The best eluent of phosphate (0.5 M NaOH) was used in all the desorption cycles. Before reuse, the regenerated sorbent was rinsed and dried. The reuse capability of regenerated PFC is shown in Fig. 3. In the fourth adsorption/desorption cycle, the PFC was able to remove 20.39% of phosphate. After regeneration, the effectiveness of PFC in removing phosphate is reduced due to the reduction of active sites of sorption [36].

Sorption kinetics, isotherm modelling, and thermodynamic studies

Sorption kinetics

The kinetics of PFC in sorbing phosphate from synthetic greywater was probed with pseudo-first-order and pseudo-second-order kinetic models. The best model was identified by the values of linear coefficient of determination (R^2) and Chi-square (χ^2). The study was conducted at pH 6.5 and sorbent dosage 3 g/L for an influent phosphate concentration of 155 mg/L.

The kinetic model parameters such as the capacity of the sorbent at equilibrium (q_e), rate constant (k_1 and k_2), and R^2 are summarised in Table 2. The maximum sorption capacity provided by the pseudo-second-order kinetic model was fairly close to the experimental value. Therefore, the phosphate sorption data of PFC were well fitted to the pseudo-second-order kinetics model. Thus, the phosphate sorption rate of PFC is dependent on adsorption capacity and not on the concentration of phosphate [31, 37]. The pseudo-second-order kinetics model of the sorbent is shown in Fig. 4A.

Adsorption isotherms

The isotherm modelling was done by fitting the phosphate sorption values with various adsorbent dosages (pH 6.5 and contact time 6 h) into Langmuir, Freundlich, and Dubinin–Radushkevich (D–R). The adsorption isotherm parameters are shown in Table 3. The Langmuir isotherm provided the value of equilibrium parameter (R_L), between 0 and 1, indicating the favourable phosphate sorption by PFC under the given conditions. The value of Freundlich adsorption coefficient (n) between 1 and 10, from the Freundlich isotherm analysis, also showed favourable phosphate sorption.

Based on the value of χ^2 and R^2, the phosphate adsorption characteristics of PFC was delineated by Langmuir isotherm (Fig. 4B). The D–R isotherm obtained a poor regression coefficient ($R^2 < 0.90$) with a higher Chi-square value. Thus,

Table 2 Kinetic model parameters for phosphate adsorption on PFC

(q_e) (mg/g) (experimental)	Pseudo-first-order model				Pseudo-second-order model			
	k_1 (1/h)	q_e (mg/g)	R^2	χ^2	k_2 (g/(mg•h))	q_e (mg/g)	R^2	χ^2
13.822	0.725	25.445	0.953	0.130	0.021	15.898	0.998	0.012
Equation	$\log(q_e - q_t) = \log(q_e) - \frac{k_1 t}{2.303}$ [31, 38]				$\frac{t}{q_t} = \frac{1}{k_2 q_e^2} + \frac{1}{q_e} t$ [31, 38]			

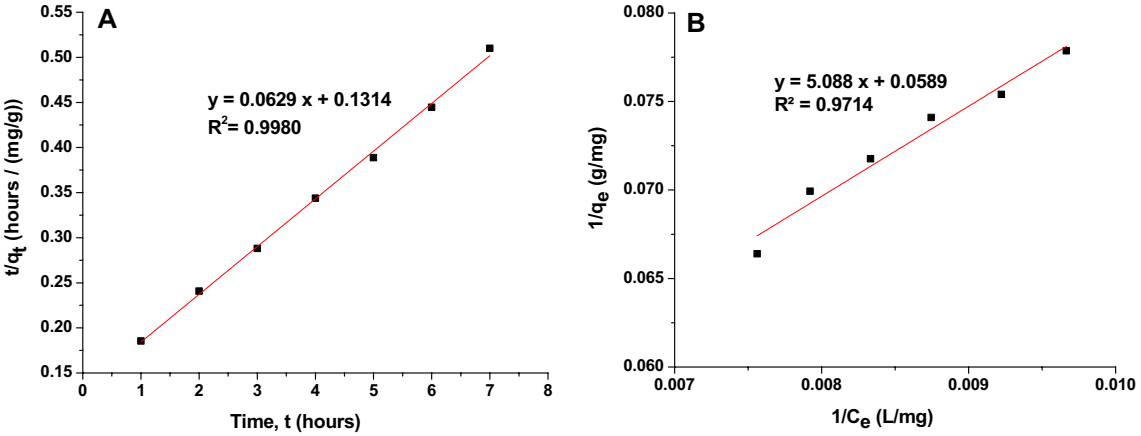

Fig. 4 **A** Pseudo-second-order kinetic model and **B** Langmuir adsorption isotherm of PFC for phosphate adsorption from synthetic greywater

Table 3 Isotherm parameters

Isotherm model	Parameters	Value	Equation
Langmuir	Q_o (mg/g)	16.9779	$\frac{1}{q_e} = \frac{1}{Q_o b} \cdot \frac{1}{C_e} + \frac{1}{Q_o}$ [15]
	b (L/mg)	0.0116	
	R_L	0.6062	
	R^2	0.9714	
	χ^2	0.0692	
Freundlich	N	1.2634	$\log q_e = \log K_f + \frac{1}{n} \log C_e$ [15]
	K_f (mg/g)(L/mg)$^{1/n}$	0.4721	
	R^2	0.9632	
	χ^2	0.0927	
D–R	β (mol^2/J^2)	0.0015	$\ln q_e = \ln q_m - \beta\epsilon^2$ [39]
	q_m (mg/g)	25.9630	
	E (kJ/mol)	0.0183	
	R^2	0.8753	
	χ^2	0.2934	

the D–R isotherm model was found unfit to describe the phosphate sorption on PFC.

Thermodynamics of phosphate adsorption by PFC

The study was conducted at three different temperatures (300 K, 310 K, and 320 K). The thermodynamic parameters like Gibbs free energy (ΔG^o), enthalpy (ΔH^o), and entropy (ΔS^o) for the adsorption of phosphate on PFC were obtained by using the Eqs. 4–7 [36]. The thermodynamic parameters are listed in Table 4.

$$\Delta G^\circ = -RT \ln K_c \tag{4}$$

$$\Delta G^\circ = \Delta H^\circ - T\Delta S^\circ \tag{5}$$

$$\ln K_c = \frac{\Delta S^\circ}{R} - \frac{\Delta H^\circ}{RT} \tag{6}$$

Table 4 Thermodynamic parameters of PFC for phosphate adsorption from greywater

Temperature (K)	ΔG^o (kJ/mol)	ΔH^o (kJ/mol)	ΔS^o (kJmol^{-1} K^{-1})
300	− 1.983	− 29.734	− 0.093
310	− 1.058		
320	− 0.133		

$$K_c = \frac{C_{Ae}}{C_e} \quad (7)$$

where K_c is the equilibrium constant of adsorption at temperature T (K), C_e is the phosphate concentration in the effluent at equilibrium (mg/L), C_{Ae} is the amount of adsorbed phosphate per litre of solution at equilibrium (mg/L), and R is the ideal gas constant (8.314 Jmol^{-1} K^{-1}). ΔH^o and ΔS^o were determined from the grade and intercept of the linear plot of lnK_c versus 1/T (Fig. 5).

The negative value of ΔG^o indicates the practicality and instinctive character of the adsorption process. The negative value for enthalpy change (ΔH^o) showed the exothermal behaviour of PFC on phosphate sorption [32]. This also indicated a reduction in phosphate adsorption capacity of PFC with increasing temperature. The negative entropy change (ΔS^o) explicated that the adsorption of phosphate on the surface of the sorbents led to an ordered phase through the formation of an activated complex between adsorbate and adsorbent [40]. The small ΔS^o value in the system under investigation revealed that no significant structural change occurred in the adsorbent material [41].

The increase in the negative value of ΔG^o with temperature showed that the adsorption process was more favourable at lower temperatures. In addition, the lower ΔG^o value (< − 20 kJ/mol) confirmed the adsorption of phosphate by PFC was favoured by physical forces [42, 43].

Mechanism of phosphate adsorption

The pathway towards phosphate sorption from synthetic greywater by PFC was determined using FTIR spectroscopy, XRD studies, and EDX analysis. The electrostatic interaction between the phosphate ions and ammonium ions resulted in the sorption of phosphate by PFC, which was established by the development of a new band at 2940.02 cm^{-1} in the FTIR spectrum of PFC after sorbing phosphate from synthetic greywater (Fig. 6). The new peak at 1371.21 cm^{-1} in the FTIR spectrum of PFC after treatment is attributed to the sorption of SO_4^{2-} ions by PFC [44].

Similar XRD patterns were exhibited by the PFC before and after phosphate adsorption (Fig. 7). This indicates its stability [45]. The escalated weight percentage of phosphorus from 0.67% (prior to the treatment) to 0.79% (post-treatment) in the EDX pattern of PFC (Fig. 8) proved the phosphate uptake. The presence of chlorine in the EDX pattern of PFC after treatment confirmed the uptake of chloride from synthetic greywater.

Regression analysis using SPSS

The relationship between independent variables (contact time (A), pH (B), and adsorbent dosage (C)) and dependent variable (phosphate sorption efficiency) was determined by regression analysis using IBM SPSS statistics 26.0 with 95% confidence interval (number of data points, 51). The

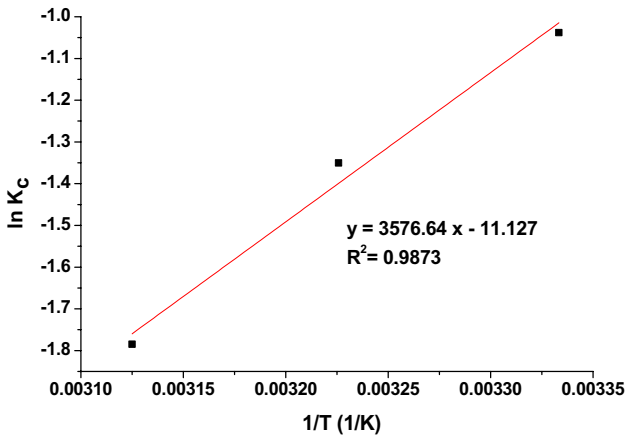

Fig. 5 Plot of lnK_c versus 1/T for phosphate sorption from greywater by PFC

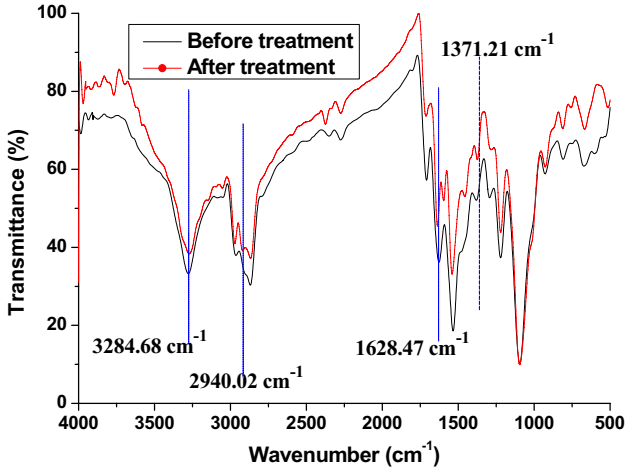

Fig. 6 FTIR spectrum of PFC before and after treatment

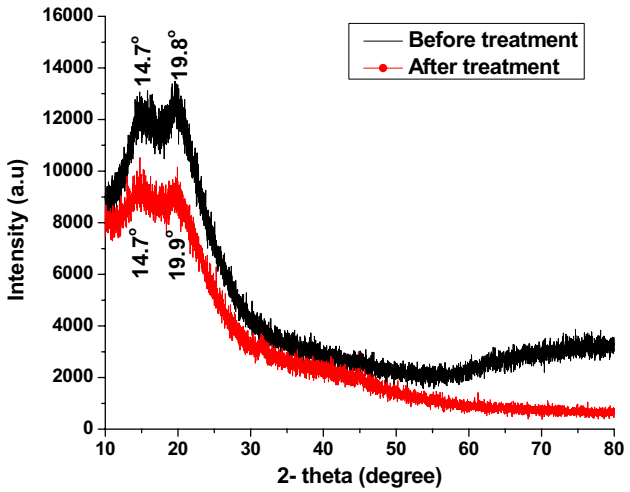

Fig. 7 XRD pattern of PFC before and after treatment

model accuracy was determined by the linear coefficient of determination (R^2) and NRMSE.

The obtained MLR model by running regression analysis (Eq. 8) expressed the high correlation between observed and predicted values with R^2 value of 0.959. The obtained equation for phosphate sorption efficiency (E_m) is

$$Em = 24.330\ logA + 93.138\ logB + 19.029\ C - 0.102\ (AB) - 1.899\ (BC) - 86.346 \quad (8)$$

The p-value (significant level) obtained from ANOVA (F-test) was < 0.05 (Table 5), which verified the good adherence of values given by the MLR model with experimental results. The values of coefficients and their significance (p-value) obtained from MLR modelling (Table S1 of supplementary material section) showed a lower p-value confirming the statistical significance of all parameters under consideration.

The NRMSE value of 0.0746 (7.46% < 10%) obtained from the regression analysis, also revealed that the predicted values by the model were in agreement with the experimental values.

Antibacterial activity of PFC

The bactericidal property of PFC and PUF was evaluated in coliform bacterial suspension (5×10^6 CFU/mL). After 24 h of incubation at 35 ± 0.5 °C, the bacterial suspension with PUF was more turbid than that with PFC. The turbidity can be related to the number of coliforms [46], and the results can be quantified by the optical density (OD) values. The absorbance of light will be more in the samples having higher bacterial concentrations [27]. The values of OD at

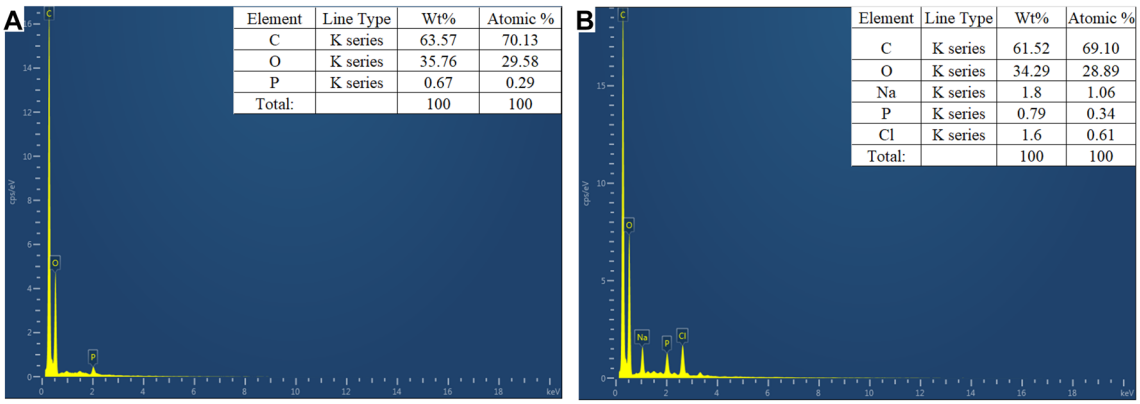

Fig. 8 EDX pattern of PFC **A** before treatment **B** after treatment

Table 5 Analysis of variance (ANOVA) for phosphate removal efficiency

Model	Sum of squares	Degree of freedom (df)	Mean square	F	Significance
Regression	2004.642	5	400.928	211.770	0.000
Residual	85.195	45	1.893		
Total	2089.838	50			

600 nm were 1.455 for the inoculated bacterial suspension, 1.390 for the inoculated bacterial suspension with PUF, and 0.327 for the inoculated bacterial suspension with PFC. This indicated that the PFC showed an inhibition efficiency of 77.53%, whereas PUF exhibited only 2.41%. The enhanced antibacterial activity of PFC can be attributed to the presence of CSNPs. The inhibition of bacterial growth by the chitosan nanoparticles is due to the binding of cationic amino groups of chitosan nanoparticles to anionic groups of microorganisms. This binding will disrupt the cell membrane and increase the cell membrane permeability leading to the death of coliform bacteria [47].

Coliform removal efficiency by PFC

The contact time and pH are considered to be the most important parameters affecting the coliform removal [48]. The evaluation of coliform removal efficacy of PFC from synthetic greywater was done by varying the pH from 5 to 9 at different contact time (0.5–3 h) with PFC dosage 3 g/L and influent coliform concentration of 38×10^3 CFU/mL at room temperature (27 °C). The coliform removal efficiency was found to increase with time for all pH until the equilibrium conditions were met (Fig. 9). The effective time needed for the CSNPs on the sorbent surface to interact with the bacterial membrane cell was found to be 1.5 h. No notable changes were observed in the removal of coliforms after 1.5 h. The results also showed that there was no significant effect of pH on the removal of coliforms by PFC. This is due to the fact that the variation of pH has no effect on intestinal bacteria like coliforms [49]. The maximum coliform removal efficiency by PFC was found to be 99.91%.

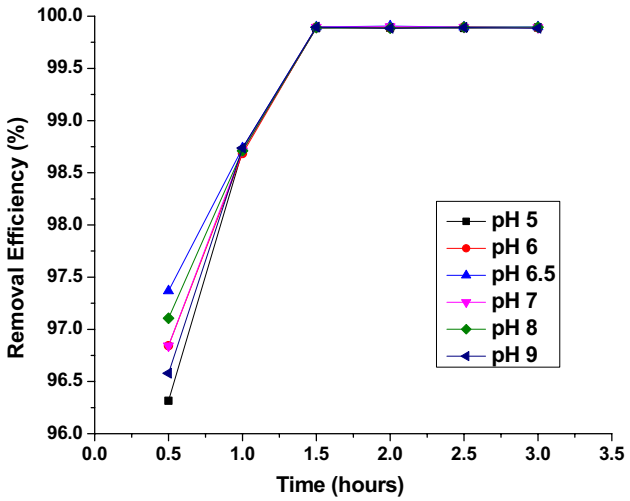

Fig. 9 Effect of pH and contact time on coliform removal by PFC

The sorbent showed better performance over downflow hanging sponge (DHS) biotower which removed 16% of phosphate (influent concentration, 12.3 mg/L) and 99.99% of coliforms (influent concentration 9.4×10^6 MPN/100 mL) [50], upflow anaerobic sludge blanket (UASB) reactor which removed 24% of phosphate (phosphate concentration, 30.36 mg/L) [51], and electrocoagulation with aluminium electrodes that removed 13.6% of phosphate (influent concentration, 2.2 mg/L) [52].

Conclusions

The study addressed the application of nanomaterials in the treatment of greywater for the first time. The phosphate sorption ability, coliform removal efficiency, and antibacterial activity of the new sorbent developed by impregnating CSNPs on polyurethane foam (PFC) were evaluated. The existence of nanoparticles on PFC was verified by the FESEM images. The EDX pattern validated the composition of nanoparticles. The FTIR analysis revealed that the phosphate sorption mechanism by PFC was due to the electrostatic interaction between the amino group and phosphate ions. The XRD analysis explained the amorphous nature of CSNPs and PUF along with the stability of PFC. The phosphate sorption was not high and the effluent failed to meet the discharge limit of 15 mg/L (5 mg P/L) as per the *E*(*P*) rules, 1986. The existence of coexisting anions and organic matter (Cl^-, SO_4^{2-}, HCO_3^- and glucose) in the synthetic greywater and the high influent phosphate concentration led to the reduced phosphate sorption efficacy of PFC. The EDX studies and FTIR analysis after treatment unmasked the affinity of PFC towards chloride and sulphate ions. The kinetic study of phosphate sorption from synthetic greywater was well described by the pseudo-second-order model and the most fitted isotherm model was Langmuir showing monolayer adsorption of phosphate. The lower value of Gibbs free energy (< -20 kJ/mol) confirmed the binding of phosphate on PFC by physical forces. The multiple linear regression model with an R^2 value of 0.959 was developed for predicting the phosphate removal efficiency by PFC.

The studies on the antibacterial activity of PFC proved its ability in inhibiting the growth of coliforms. PFC can effectively remove coliform bacteria from synthetic greywater without significant changes in efficiency at varying pH from 5 to 9. Thus, no pH adjustment is required, a unique advantage for its application as disinfectant in greywater/wastewater treatment.

The performance of PFC in removing phosphate and coliforms from greywater outpaced the biological treatment systems like UASB and DHS biotower. The potential of PFC as a phosphate sorbent and as a bactericidal agent can be enhanced by the addition of metal nanoparticles (silver,

copper, zinc, etc.) which are found to have good antibacterial activity and attraction towards phosphate ions. Also, the pre-treatment of wastewater to remove competing ions like chlorides, sulphates, etc. before the sorption of phosphate by PFC can improve the phosphate removal efficacy.

Supplementary Information The online version contains supplementary material available at https://doi.org/10.1007/s41204-021-00214-0.

Acknowledgements The authors would like to thank the laboratory staff and co-researcher at Government Engineering College, Thrissur, Kerala, for their help and support. The facilities arranged by the Centre for Materials for Electronics Technology, Thrissur, and Sophisticated Test and Instrumentation Centre, Cochin, as part of characterisation studies are strongly appreciated.

Authors contributions Conceptualisation, methodology, formal analysis and investigation, and writing the original draft were executed by Anjali P. Sasidharan. Supervision, writing, reviewing, and editing were completed by Meera V and Vinod P. Raphael. All authors read the manuscript and approved.

Funding The authors did not receive any financial support for the submitted work.

Availability of data and material This research paper and supplementary materials contain all the data generated or analysed during this study.

Declarations

Consent to participate Not applicable.

Consent for publication Not applicable.

Conflict of interest The authors declare that they have no potential competing interests.

Ethics approval This article does not contain any studies with human participants or animals performed by any of the authors.

References

1. Soo C, Ling T, Lee N, Apun K (2016) Assessment of the characteristic of nutrients, total metals, and fecal coliform in Sibu Laut River, Sarawak, Malaysia. Appl Water Sci 6:77–96. https://doi.org/10.1007/s13201-014-0205-7
2. Praveena VD, Kumar KV, Venkataratnam K (2016) Phosphate removal from aqueous solutions by a nanostructured Ag–Chitosan film. J Nanosci Technol 2:134–137
3. Mekonnen DT, Alemayehu E, Lennartz B (2021) Adsorptive removal of phosphate from aqueous solutions using low-cost volcanic rocks: kinetics and equillibrium approaches. Materials (Basel) 14:1–16
4. Huang W, Zhang Y, Li D (2017) Adsorptive removal of phosphate from water using mesoporous materials: a review. J Environ Manag 193:470–482. https://doi.org/10.1016/j.jenvman.2017.02.030
5. Pokhrel MR, Poudel BR, Aryal RL, Paudyal H, Ghimire KN (2019) Removal and recovery of phosphate from water and wastewater using metal-loaded agricultural waste-based adsorbents: a review. J Inst Sci Technol 24:77–89. https://doi.org/10.3126/jist.v24i1.24640
6. Pachepsky YA, Allende A, Boithias L, Cho K, Jamieson R, Hofstra N, Molina M (2018) Microbial water quality: monitoring and modeling. J Environ Qual 47:931–938. https://doi.org/10.2134/jeq2018.07.0277
7. Mazhar MA, Khan NA, Ahmed S, Khan AH, Hussain A, Rahisuddin CF, Yousef M, Ahmadi S, Vambol V (2020) Chlorination disinfection by-products in municipal drinking water—a review. J Clean Prod. https://doi.org/10.1016/j.jclepro.2020.123159
8. Elhegazy H, Eid MMM (2020) A state-of-the-art-review on greywater management: a survey from 2000 to 2020s. Water Sci Technol 82:2786–2797. https://doi.org/10.2166/wst.2020.549
9. Rahdar S, Rahdar A, Sattari M, Hafshejani LD, Tolkou AK, Kyzas GZ (2021) Barium/Cobalt@Polyethylene glycol nanocomposites for dye removal from aqueous solution. Polymers (Basel) 13:1–19. https://doi.org/10.3390/polym13071161
10. Mohammadi L, Rahdar A, Khaksefidi R, Ghambkhari A, Fytianos G, Kyzas GZ (2020) Polystyrene magnetic nanocomposites as antibiotic adsorbents. Polymers (Basel) 12:1–18. https://doi.org/10.3390/polym12061313
11. Trinh VT, Nguyen TMP, Van HT, Hoang LP, Nguyen TV, Ha LT, Vu XH, Pham TT, Nguyen TN, Quang NV, Nguyen XC (2020) Phosphate adsorption by silver nanoparticles-loaded activated carbon derived from tea residue. Sci Rep 10:1–13. https://doi.org/10.1038/s41598-020-60542-0
12. Rahdar A, Rahdar S, Labuto G (2020) Environmentally friendly synthesis of Fe_2O_3@SiO_2 nanocomposite: characterization and application as an adsorbent to aniline removal from aqueous solution. Environ Sci Pollut Res 27:9181–9191. https://doi.org/10.1007/s11356-019-07491-y
13. Rahdar A, Rahdar S, Askari F, Ahmadi S, Shahraki H, Mohammadi L, Sivasankarapillai VS, Kyzas GZ (2021) Effectiveness of graphene quantum dot nanoparticles in the presence of hydrogen peroxide for the removal of ciprofloxacin from aqueous media: response surface methodology. Sep Sci Technol 56:2124–2140. https://doi.org/10.1080/01496395.2020.1807569
14. Yanat M, Schroën K (2021) Preparation methods and applications of chitosan nanoparticles; with an outlook toward reinforcement of biodegradable packaging. React Funct Polym 161:1–12. https://doi.org/10.1016/j.reactfunctpolym.2021.104849
15. Sivakami MS, Gomathi T, Venkatesan J, Jeong H, Kim S, Sudha PN (2013) Preparation and characterization of nano chitosan for treatment wastewaters. Int J Biol Macromol 57:204–212. https://doi.org/10.1016/j.ijbiomac.2013.03.005
16. Gokila S, Gomathi T, Sudha PN, Anil S (2017) Removal of the heavy metal ion chromium(VI) using Chitosan and Alginate nanocomposites. Int J Biol Macromol 104:1459–1468. https://doi.org/10.1016/j.ijbiomac.2017.05.117
17. Hua M, Zhang S, Pan B, Zhang W, Lv L, Zhang Q (2012) Heavy metal removal from water/wastewater by nanosized metal oxides: a review. J Hazard Mater 211–212:317–331. https://doi.org/10.1016/j.jhazmat.2011.10.016
18. Phong NTP, Thanh NVK, Phuong PH (2009) Fabrication of antibacterial water filter by coating silver nanoparticles on flexible polyurethane foams. J Phys Conf Ser 187:1–8. https://doi.org/10.1088/1742-6596/187/1/012079
19. Jain P, Pradeep T (2005) Potential of silver nanoparticle-coated polyurethane foam as an antibacterial water filter. Biotechnol Bioeng 90:3–7. https://doi.org/10.1002/bit.20368
20. Anjali PS, Meera V, Vinod PR (2021) Efficacy of nanochitosan impregnated polyurethane foam in removing phosphate from aqueous solutions. IOP Conf Ser Mater Sci Eng 1114:1–8. https://doi.org/10.1088/1757-899x/1114/1/012083

21. Agarwal M, Agarwal MK, Shrivastav N, Pandey S, Das R, Gaur P (2018) Preparation of chitosan nanoparticles and their in-vitro characterization. Int J Life-Sci Sci Res 4:1713–1720. https://doi.org/10.21276/ijlssr.2018.4.2.17
22. Anand M, Sathyapriya P, Maruthupandy M, Hameedha Beevi A (2018) Synthesis of chitosan nanoparticles by TPP and their potential mosquito larvicidal application. Front Lab Med 2:72–78. https://doi.org/10.1016/j.flm.2018.07.003
23. Centenaro GSNM, Facin BR, Valério A, de Souza AAU, da Silva A, de Oliveira JV, de Oliveira D (2017) Application of polyurethane foam chitosan-coated as a low-cost adsorbent in the effluent treatment. J Water Process Eng 20:201–206. https://doi.org/10.1016/j.jwpe.2017.11.008
24. Khan MSJ, Kamal T, Ali F, Asiri AM, Khan SB (2019) Chitosan-coated polyurethane sponge supported metal nanoparticles for catalytic reduction of organic pollutants. Int J Biol Macromol 132:772–783. https://doi.org/10.1016/j.ijbiomac.2019.03.205
25. Abed SN, Scholz M (2016) Chemical simulation of greywater. Environ Technol (U K) 37:1631–1646. https://doi.org/10.1080/09593330.2015.1123301
26. Bahrami M, Amiri MJ, Mahmoudi MR, Koochaki S (2017) Modeling caffeine adsorption by multi-walled carbon nanotubes using multiple polynomial regression with interaction effects. J Water Health 15:526–535. https://doi.org/10.2166/wh.2017.297
27. Waheed S, Ahmad A, Maqsood SK, Gul S, Jamil T, Islam A, Hussain T (2014) Synthesis, characterization, permeation and antibacterial properties of cellulose acetate/polyethylene glycol membranes modified with chitosan. Desalination 351:59–69. https://doi.org/10.1016/j.desal.2014.07.019
28. APHA AW (2017) Standard methods for the examination of water and wastewater, 23rd edition. Am. Public Heal. Assoc. (APHA), Am. Water Work. Assoc. (AWWA), Water Environ. Fed. (WEF), Washingt. DC, USA
29. Liu R, Chi L, Wang X, Sui Y, Wang Y, Arandiyan H (2018) Review of metal (Hydr) oxide and other adsorptive materials for phosphate removal from water. J Environ Chem Eng 6:5269–5286. https://doi.org/10.1016/j.jece.2018.08.008
30. Chukwuemeka-Okorie HO, Ekuma FK, Akpomie KG, Nnaj JC, Okereafor AG (2021) Adsorption of tartrazine and sunset yellow anionic dyes onto activated carbon derived from cassava sievate biomass. Appl Water Sci 11:1–8. https://doi.org/10.1007/s13201-021-01357-w
31. Rahdar S, Pal K, Mohammadi L, Goharniya Y, Samani S, Kyzas GZ (2021) Response surface methodology for the removal of nitrate ions by adsorption onto copper oxide nanoparticles. J Mol Struct 1231:129686. https://doi.org/10.1016/j.molstruc.2020.129686
32. Sowmya A, Meenakshi S (2014) Effective removal of nitrate and phosphate anions from aqueous solutions using functionalised chitosan beads. Desalin Water Treat 52:2583–2593. https://doi.org/10.1080/19443994.2013.798842
33. Lǔ J, Liu H, Liu R, Zhao X, Sun L, Qu J (2013) Adsorptive removal of phosphate by a nanostructured Fe–Al–Mn tri-metal oxide adsorbent. Powder Technol 233:146–154. https://doi.org/10.1016/j.powtec.2012.08.024
34. Li M, Liu J, Xu Y, Qian G (2016) Phosphate adsorption on metal oxides and metal hydroxides: a comparative review. Environ Rev 24:319–332. https://doi.org/10.1139/er-2015-0080
35. Abd-Elhakeem MA, Ramadan M, Basaad SF (2016) Removing of heavy metals from water by chitosan nanoparticles. J Adv Chem 11:3765–3771. https://doi.org/10.24297/jac.v11i7.2200
36. Ajmal Z, Muhmood A, Usman M, Kizito S, Lu J, Dong R, Wu S (2018) Phosphate removal from aqueous solution using iron oxides: adsorption, desorption and regeneration characteristics. J Colloid Interface Sci 528:145–155. https://doi.org/10.1016/j.jcis.2018.05.084
37. Sahoo TR, Prelot B (2020) Adsorption processes for the removal of contaminants from wastewater. Elsevier, Amsterdam
38. Yao S, Wang M, Liu J, Tang S, Chen H, Guo T, Yang G, Yao C (2018) Removal of phosphate from aqueous solution by sewage sludge-based activated carbon loaded with pyrolusite. J Water Reuse Desalin 8:192–201. https://doi.org/10.2166/wrd.2017.054
39. Barathi M, Santhana Krishna Kumar A, Rajesh N (2013) Efficacy of novel Al-Zr impregnated cellulose adsorbent prepared using microwave irradiation for the facile defluoridation of water. J Environ Chem Eng 1:1325–1335. https://doi.org/10.1016/j.jece.2013.09.026
40. Du X, Wu T, Sun F, Hou Z, Liu Z, Huo L, Hao Y, Zhao Y (2019) Adsorption equilibrium and thermodynamic analysis of CO2 and CH4 on Qinshui Basin anthracite. Geofluids. https://doi.org/10.1155/2019/8268050
41. Sahmoune MN (2019) Evaluation of thermodynamic parameters for adsorption of heavy metals by green adsorbents. Environ Chem Lett 17:697–704. https://doi.org/10.1007/s10311-018-00819-z
42. Húmpola PD, Odetti HS, Fertitta AE, Vicente JL (2013) Thermodynamic analysis of adsorption models of phenol in liquid phase on different activated carbons. J Chil Chem Soc 58:1541–1544. https://doi.org/10.4067/S0717-97072013000100009
43. Saha P, Chowdhury S (2011) Insight into adsorption thermodynamics. In: Thermodynamics. InTech, ISBN: 978-953-307-544-0. http://www.intechopen.com/books/thermodynamics/insight-into-adsorption-thermodynamics
44. Pavia DL, Lampman GM, Kriz GS, Vyvyan JR (2013) Introduction to spectroscopy. In: Fifth edition. pp 1–786
45. Fu F, Cheng Z, Dionysiou DD, Tang B (2015) Fe/Al bimetallic particles for the fast and highly efficient removal of Cr(VI) over a wide pH range: performance and mechanism. J Hazard Mater 298:261–269. https://doi.org/10.1016/j.jhazmat.2015.05.047
46. Farrell C, Hassard F, Jefferson B et al (2018) Turbidity composition and the relationship with microbial attachment and UV inactivation efficacy. Sci Total Environ 624:638–647. https://doi.org/10.1016/j.scitotenv.2017.12.173
47. Rozman NAS, Yenn TW, Ring LC et al (2019) Potential antimicrobial applications of chitosan nanoparticles (ChNP). J Microbiol Biotechnol 29:1009–1013. https://doi.org/10.4014/jmb.1904.04065
48. Ghamkhari A, Mohamadi L, Kazemzadeh S, Zafar MN, Rahdar A, Khaksefidi R (2020) Synthesis and characterization of poly(styrene-block-acrylic acid) diblock copolymer modified magnetite nanocomposite for efficient removal of penicillin G. Compos (Part B). https://doi.org/10.1016/j.compositesb.2019.107643
49. Asadi S, Moeinpour F (2019) Inactivation of Escherichia coli in water by silver-coated Ni0.5Zn0.5Fe2O4 magnetic nanocomposite: a Box-Behnken design optimization. Appl Water Sci 9:1–9. https://doi.org/10.1007/s13201-019-0901-4
50. Mahmoud M, Tawfik A, Samhan F, El-Gohary F (2009) Sewage treatment using an integrated system consisting of anaerobic hybrid reactor (AHR) and downflow hanging sponge (DHS). Desalin Water Treat 4:168–176. https://doi.org/10.5004/dwt.2009.372
51. Elmitwalli TA, Shalabi M, Wendland C, Otterpohl R (2007) Greywater treatment in UASB reactor at ambient temperature. Water Sci Technol 55:173–180. https://doi.org/10.2166/wst.2007.142
52. Nasr M, Ateia M, Hassan K (2016) Artificial intelligence for greywater treatment using electrocoagulation process. Sep Sci Technol 51:96–105. https://doi.org/10.1080/01496395.2015.1062399